Matter and Radiation at Extremes | RESEARCH ARTICLE | scitation.org/journal/mre

Collective stimulated Brillouin scattering modes of two crossing laser beams with shared scattered wave

Cite as: Matter Radiat. Extremes 6, 065903 (2021); doi: 10.1063/5.0062902
Submitted: 9 July 2021 • Accepted: 10 September 2021 •
Published Online: 11 October 2021

Jie Qiu,[1] Liang Hao,[1,a)] Lihua Cao,[1,2] and Shiyang Zou[1]

AFFILIATIONS

[1]Institute of Applied Physics and Computational Mathematics, Beijing 100094, China
[2]HEDPS, Center for Applied Physics and Technology, Peking University, Beijing 100871, China

[a)]**Author to whom correspondence should be addressed:** hao_liang@iapcm.ac.cn

ABSTRACT

In inertial confinement fusion (ICF), overlapping of laser beams is common. Owing to the effective high laser intensity of the overlapped beams, the collective mode of stimulated Brillouin scattering (SBS) with a shared scattered light wave is potentially important. In this work, an exact analytic solution for the convective gain coefficient of the collective SBS modes with shared scattered wave is presented for two overlapped beams based on a linear kinetic model. The effects of the crossing angle, polarization states, and finite beam overlapping volume of the two laser beams on the shared light modes are analyzed for cases with zero and nonzero wavelength difference between the two beams. It is found that all these factors have a significant influence on the shared light modes of SBS. Furthermore, the out-of-plane modes, in which the wavevectors of daughter waves lie in different planes from the two overlapped beams, are found to be important for certain polarization states and especially for obtuse crossing angles. In particular, adjusting the polarization directions of the two beams to be orthogonal to each other or tuning the wavelength difference to a sufficiently large value (of the order of nanometers) are found to be effective methods to suppress the shared light modes of SBS. This work will be helpful for comprehending and suppressing collective SBS with shared scattered waves in ICF experiments.

I. INTRODUCTION

In inertial confinement fusion (ICF), owing to the limited energy of a single laser beam, a large number of beams are needed to deliver the megajoule laser energy to the target required for both indirect-drive and direct-drive schemes.[1–3] The ubiquitous overlapping of laser beams leads to complex multibeam laser–plasma interaction (LPI) instabilities, including crossed-beam energy transfer (CBET) between different beams,[4–8] seeded multibeam instability due to seeds generated elsewhere in the plasma[1] and by glint,[9] and collective instability with shared daughter waves.[3,10,11] Among the various LPI instabilities in ICF, stimulated Brillouin scattering (SBS) and stimulated Raman scattering (SRS) instabilities are of primary concern, since they can scatter significant amounts of light, leading to a great energy loss from the incident lasers as well as degradation of the irradiation symmetry.[12–17] The collective modes with common daughter waves deserve particular attention owing to their great temporal growth rate and convective gain, which scale up with the number of pump beams.[18–20] Experimentally, collective SRS and SBS result in significant scattered light losses in novel directions,[19–21] which can be located far from the apertures of the beams where diagnostics are usually set up[12,22] and are hence quite hard to detect. Understanding these processes is essential for better identifying, modeling, and diagnosing multibeam SRS or SBS processes and is helpful to optimize ICF implosions.

The collective SRS or SBS processes include shared plasma (SP) wave modes and shared light (SL) wave modes, depending on whether the shared daughter wave is a common Langmuir/ion acoustic wave or a common scattered wave. Previous theoretical studies of the homogeneous temporal growth rate for collective SP and SL modes of multiple beams have been conducted using a fluid description.[23–25] In addition, some two-dimensional (2D) particle-in-cell simulations have verified the importance of in-plane collective SRS modes of two overlapped beams,[25,26] where the wavevectors of daughter waves lie in the plane of incidence of two overlapped beams. The SP modes of collective SBS in the spatial convective regime, which is typical of practical ICF conditions,[27–29] have recently been studied, and it has been found that the out-of-plane modes can be quite important for some polarization states of the laser beams.[30] In the present work, the SL modes of collective SBS in the convective regime are studied, and the impacts of the crossing angle, polarization states, and finite beam overlapping volume of the two laser beams on SL modes of SBS are investigated systematically for both zero and nonzero wavelength differences between the two pump beams. Compared with the SP modes, the SL modes are found to be much more sensitive to the polarization states and wavelength difference. Nevertheless, the out-of-plane modes can still be quite important for some polarization states and beam crossing angles. The results of this work should be helpful in comprehending and estimating the importance of collective SBS with shared scattered wave in ICF experiments.

The remainder of the paper is organized as follows. In Sec. II, the theoretical model for SL modes is presented, where an analytic solution for the convective gain coefficient is given. In Sec. III, the impacts of the crossing angle, polarization states, and finite beam overlapping volume of the two laser beams on the scattered wavelength and spatial amplification of the collective SBS modes with shared scattered wave are investigated for both zero and nonzero wavelength differences between the pump lasers, and the importance of out-of-plane modes relative to in-plane modes is discussed. In Sec. IV, the conclusions are given, together with some discussions.

II. THEORETICAL MODEL FOR SL MODES OF TWO CROSSING BEAMS

The SL modes of two crossing beams incorporate five coupled waves: the two pump light waves and one common scattered light wave, as well as two plasma waves corresponding to the coupling between each pump light and the common scattered light. The phase matching conditions can be written as

$$\omega_{0\alpha} = \omega_{\rm s} + \omega_{es_\alpha}, \tag{1}$$

$$\mathbf{k}_{0\alpha} = \mathbf{k}_{\rm s} + \mathbf{k}_{es_\alpha}, \tag{2}$$

where the ω_i with subscripts $i = 0\alpha$, es$_\alpha$, and s ($\alpha = 1, 2$) are the wave frequencies of laser beam α, plasma wave α, and the common scattered wave, respectively, and $\mathbf{k}_i$ with $i = 0\alpha$, es$_\alpha$, and s are the corresponding wavevectors. The geometry of the collective SL modes for two overlapped beams with crossing angle $2\theta_{\rm h}$ is shown in Fig. 1(a), where the xy plane is defined as the $(\mathbf{k}_{01}, \mathbf{k}_{02})$ plane with the x direction along the bisector of $\mathbf{k}_{01}$ and $\mathbf{k}_{02}$. The direction of the wavevector $\mathbf{k}_{\rm s}$ for the scattered wave can be specified by $(\theta_{\rm s}, \varphi_{\rm s})$, where the out-of-plane angle $-90^\circ \le \varphi_{\rm s} \le 90^\circ$ is the altitude of $\mathbf{k}_{\rm s}$ measured from the xy plane, and the azimuthal angle $-180^\circ \le \theta_{\rm s} \le 180^\circ$ is the angle from the x axis to the orthogonal projection of $\mathbf{k}_{\rm s}$ onto the xy

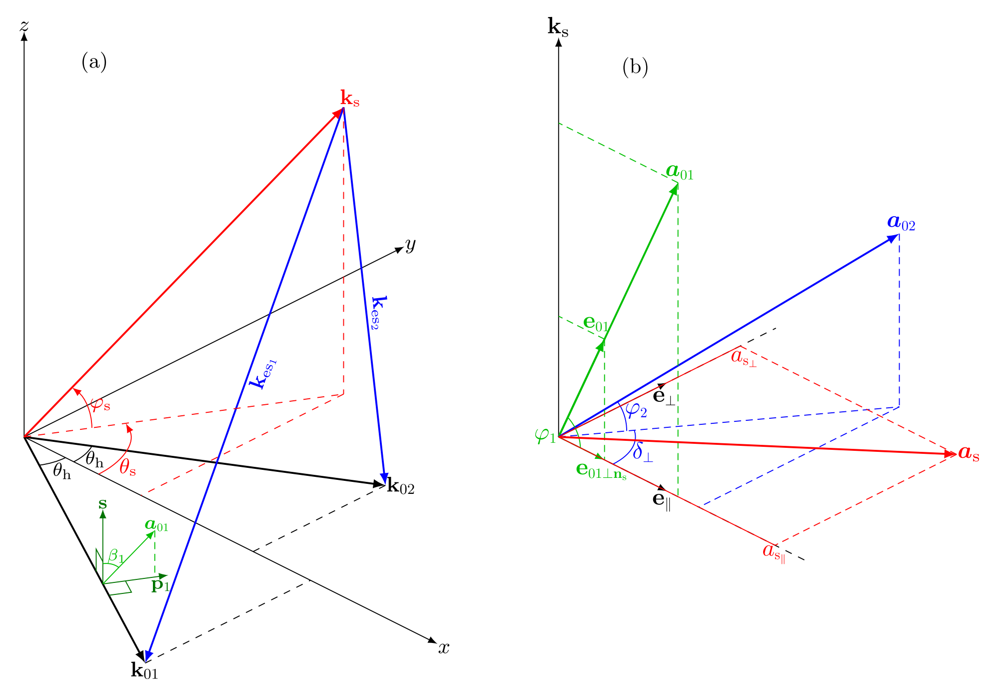

FIG. 1. (a) Geometry of collective SL modes for two overlapped beams. (For generality, a nonzero wavelength difference of these two beams is assumed.) In the presented coordinate system, the xy plane is chosen to be the $(\mathbf{k}_{01}, \mathbf{k}_{02})$ plane with the x axis along the bisector of $\mathbf{k}_{01}$ and $\mathbf{k}_{02}$ and the z axis along $\mathbf{k}_{01} \times \mathbf{k}_{02}$. Beam I or beam II is said to be s-polarized when $\pm\boldsymbol{a}_{0\alpha}$ is along the $\mathbf{s}$ (z-axis) direction and to be p-polarized when $\pm\boldsymbol{a}_{0\alpha}\|\mathbf{p}_\alpha$ is located in the xy plane. Other linear polarization states of beam I or II are described by the polarization angle $90^\circ \ge \beta_\alpha \ge -90^\circ$, which is the angle from $\mathbf{s}$ to $\pm\boldsymbol{a}_{0\alpha}$. (b) Relative orientation between the polarization directions of the two laser beams and the scattered light, where $\boldsymbol{a}_{\rm s}$ is confined within the plane perpendicular to $\mathbf{k}_{\rm s}$ (the polarization plane of the scattered light), and the angle between $\boldsymbol{a}_{0\alpha}$ and this polarization plane is φ_α. On this polarization plane, $\mathbf{e}_\|$ is defined as the unit vector along the projection of $\boldsymbol{a}_{01}$, $\mathbf{e}_\perp$ is a unit vector perpendicular to $\mathbf{e}_\|$, and the angle between the projection of $\boldsymbol{a}_{01}$ and $\boldsymbol{a}_{02}$ is $\delta_\perp$.

plane. The wavevector $\mathbf{k}_{es_\alpha}$ for the plasma wave driven by beam α is determined by the matching condition $\mathbf{k}_{es_\alpha} = \mathbf{k}_{0\alpha} - \mathbf{k}_s$, yielding

$$\begin{aligned} k_{\mathrm{es}_1} &= \sqrt{k_{01}^2 + k_s^2 - 2\mathbf{k}_{01}\cdot\mathbf{k}_s} \approx 2k_{01}\sin\frac{1}{2}\vartheta_1, \\ k_{\mathrm{es}_2} &= \sqrt{k_{02}^2 + k_s^2 - 2\mathbf{k}_{02}\cdot\mathbf{k}_s} \approx 2k_{02}\sin\frac{1}{2}\vartheta_2, \end{aligned} \tag{3}$$

where the approximate equality is applicable for collective SBS modes with a common scattered wave since $k_s \approx k_{01} \approx k_{02}$ is taken for this approximation. ϑ_1 and ϑ_2 are the scattering angles of beams I and II and are defined by

$$\begin{aligned} \cos\vartheta_1 &= \frac{\mathbf{k}_{01}\cdot\mathbf{k}_s}{k_{01}k_s} = \cos\varphi_s\cos(\theta_s+\theta_h), \\ \cos\vartheta_2 &= \frac{\mathbf{k}_{02}\cdot\mathbf{k}_s}{k_{02}k_s} = \cos\varphi_s\cos(\theta_s-\theta_h). \end{aligned} \tag{4}$$

For most practical cases in ICF, both SRS and SBS are spatial problems,[27,31,32] for which the convective amplification properties are of great importance. To study the convective amplification of the SL modes, the envelope approximation for the five coupled waves can be adopted. In the strong-damping regime, the equations for the complex vector amplitudes of the laser beams ($\boldsymbol{a}_{0\alpha}$) and the common scattered wave ($\boldsymbol{a}_s$), and for the complex amplitude of the density perturbation of plasma waves (δn_{es_α}) can be written as[30,31]

$$\frac{\delta n_{es_\alpha}}{n_0} = -\gamma_{pm_\alpha}\frac{k_{es_\alpha}^2 c^2}{2\omega_{\mathrm{pe}}^2}\boldsymbol{a}_{0\alpha}\cdot\boldsymbol{a}_s^* \tag{5}$$

and

$$\mathbf{k}_s\cdot\nabla\boldsymbol{a}_s = -\frac{j\omega_{\mathrm{pe}}^2}{4c^2}\sum_{\alpha=1,2}\frac{\delta n_{es_\alpha}^*}{n_0}a_{0\alpha}\mathbf{e}_{0\alpha\perp\mathbf{n}_s}, \tag{6}$$

where $\boldsymbol{a}_i \equiv e\mathbf{A}_i/m_e c$ is the normalization of the magnetic vector potential $\mathbf{A}$, e is the electron charge, m_e is the electron mass, n_0 is the unperturbed electron density, and c is the speed of light in vacuum. $\mathbf{e}_{0\alpha\perp\mathbf{n}_s} \equiv \mathbf{n}_s\times(\mathbf{e}_{0\alpha}\times\mathbf{n}_s) = \mathbf{e}_{0\alpha} - (\mathbf{e}_{0\alpha}\cdot\mathbf{n}_s)\mathbf{n}_s$ is the projection of $\mathbf{e}_{0\alpha} \equiv \boldsymbol{a}_{0\alpha}/a_{0\alpha}$ onto the plane perpendicular to $\mathbf{n}_s \equiv \mathbf{k}_s/k_s$, which arises because only this component of $\boldsymbol{a}_{0\alpha}$ can excite the electromagnetic component (perpendicular to $\mathbf{n}_s$) of the scattered wave. γ_{pm_α} is the ponderomotive response function[33] for plasma wave α, defined as

$$\gamma_{\mathrm{pm}}(\omega_{\mathrm{es}}, k_{\mathrm{es}}) = \frac{(1+\chi_I)\chi_e}{1+\chi_I+\chi_e}, \tag{7}$$

where $\chi_I(\omega_{es}, k_{es}) = \Sigma_\beta\chi_{i\beta}(\omega_{es}, k_{es})$ and $\chi_e(\omega_{es}, k_{es})$ are the ion susceptibility (summed over ion species β) and electron susceptibility,[34] respectively. In this paper, for simplicity, the flow velocity is assumed to be zero for all species. Nevertheless, if species β were to flow with velocity $\mathbf{u}_\beta$, then this nonzero flow velocity could easily be considered by replacing ω_{es} in $\chi_{i\beta}(\omega_{es}, k_{es})$ with $\omega_{es} - \mathbf{k}_{es}\cdot\mathbf{u}_\beta$.[35]

As illustrated in Fig. 1(b), the projections of the polarization directions $\mathbf{e}_{01}$ and $\mathbf{e}_{02}$ onto the plane perpendicular to $\mathbf{k}_s$ can be different in direction, and then, according to Eq. (6), the direction of $\boldsymbol{a}_s$ depends on the competition between the drives by beams I and II. Defining $\mathbf{e}_\parallel$ as the unit vector parallel to $\mathbf{e}_{01\perp\mathbf{n}_s}$, and $\mathbf{e}_\perp \equiv \mathbf{n}_s\times\mathbf{e}_\parallel$ as the unit vector perpendicular to $\mathbf{e}_\parallel$ and $\mathbf{n}_s$, as shown in Fig. 1(b), and writing $\boldsymbol{a}_s = a_{s_\parallel}\mathbf{e}_\parallel + a_{s_\perp}\mathbf{e}_\perp$, Eqs. (5) and (6) can be written as

$$\frac{\delta n_{\mathrm{es}_1}}{n_0} = -\gamma_{\mathrm{pm}_1}\frac{k_{\mathrm{es}_1}^2 c^2}{2\omega_{\mathrm{pe}}^2}a_{01}a_{s_\parallel}^*\cos\varphi_1, \tag{8}$$

$$\frac{\delta n_{\mathrm{es}_2}}{n_0} = -\gamma_{\mathrm{pm}_2}\frac{k_{\mathrm{es}_2}^2 c^2}{2\omega_{\mathrm{pe}}^2}a_{02}\cos\varphi_2\,(a_{s_\parallel}^*\cos\delta_\perp + a_{s_\perp}^*\sin\delta_\perp) \tag{9}$$

and

$$\mathbf{k}_s\cdot\nabla a_{s_\parallel} = -\frac{j\omega_{\mathrm{pe}}^2}{4c^2 n_0}(\delta n_{\mathrm{es}_1}^* a_{01}\cos\varphi_1 + \delta n_{\mathrm{es}_2}^* a_{02}\cos\varphi_2\cos\delta_\perp), \tag{10}$$

$$\mathbf{k}_s\cdot\nabla a_{s_\perp} = -\frac{j\omega_{\mathrm{pe}}^2}{4c^2}\frac{\delta n_{\mathrm{es}_2}^*}{n_0}a_{02}\cos\varphi_2\sin\delta_\perp, \tag{11}$$

where φ_α is the angle between $\mathbf{e}_{0\alpha\perp\mathbf{n}_s}$ and $\mathbf{e}_{0\alpha}$, which satisfies $\cos\varphi_\alpha = |\mathbf{e}_{0\alpha}\times\mathbf{n}_s|$, and $\delta_\perp$ is the angle between $\mathbf{e}_{01\perp\mathbf{n}_s}$ and $\mathbf{e}_{02\perp\mathbf{n}_s}$, which satisfies

$$\sin\delta_\perp = \frac{\mathbf{n}_s\cdot(\mathbf{e}_{01}\times\mathbf{e}_{02})}{\cos\varphi_1\cos\varphi_2}. \tag{12}$$

Inserting Eqs. (8) and (9) into Eqs. (10) and (11), equations for $a_{s_\parallel}$ and $a_{s_\perp}$ can be obtained as

$$\partial_\eta a_{s_\parallel} = \kappa_1 a_{s_\parallel} + \kappa_2\cos\delta_\perp(a_{s_\parallel}\cos\delta_\perp + a_{s_\perp}\sin\delta_\perp), \tag{13}$$

$$\partial_\eta a_{s_\perp} = \kappa_2\sin\delta_\perp(a_{s_\parallel}\cos\delta_\perp + a_{s_\perp}\sin\delta_\perp), \tag{14}$$

where the coordinate η is along the direction of $\mathbf{k}_s$, and the single-beam gain coefficients are $\kappa_1 \equiv \mathrm{Im}[\gamma_{\mathrm{pm}_1}]k_{\mathrm{es}_1}^2|a_{01}|^2\cos^2\varphi_1/8k_s$ and $\kappa_2 \equiv \mathrm{Im}[\gamma_{\mathrm{pm}_2}]k_{\mathrm{es}_2}^2|a_{02}|^2\cos^2\varphi_2/8k_s$. The gain coefficient κ_c of the common scattered wave can be obtained from Eqs. (13) and (14) by taking the solution form $a_{s_\parallel}, a_{s_\perp} \propto e^{\kappa_c\eta}$, yielding

$$\kappa_c^2 - \kappa_c(\kappa_1+\kappa_2) + \kappa_1\kappa_2\sin^2\delta_\perp = 0. \tag{15}$$

Usually, there are two solutions for κ_c, with the larger one satisfying $\max[\kappa_1, \kappa_2] \le \kappa_c \le \kappa_1 + \kappa_2$ and the smaller one satisfying $0 \le \kappa_c \le \min[\kappa_1, \kappa_2]$. The polarization directions of $\boldsymbol{a}_s$ corresponding to these two modes are orthogonal to each other and are determined by

$$\frac{a_{s_\perp}}{a_{s_\parallel}} = \frac{\kappa_2\cos\delta_\perp\sin\delta_\perp}{\kappa_c - \kappa_2\sin^2\delta_\perp}. \tag{16}$$

The mode with larger κ_c will dominate the convective amplification of the scattered wave, except when the polarization direction of the seed for $\boldsymbol{a}_s$ is exactly along the polarization direction of the mode with smaller κ_c. Therefore, it is the SL mode with larger κ_c that is mainly discussed in this work.

III. COLLECTIVE SBS MODES WITH SHARED SCATTERED WAVE FOR TWO OVERLAPPED BEAMS

In this section, we investigate the impacts of crossing angle, polarization states, and the finite overlapping volume of the two laser beams on collective SBS modes with shared scattered wave for both zero and nonzero wavelength differences between the two pump beams.

Assuming zero flow velocity, the ion acoustic waves satisfy the dispersion relation $\omega_{a_\alpha} = k_{a_\alpha}c_s$, where c_s is the ion acoustic velocity. (Note that in the context of SBS, the subscript "a" is used to denote quantities related to ion acoustic waves, which corresponds to the symbol "es" for plasma waves in Sec. II.) Then, from the matching condition

$$\omega_s = \omega_{01} - \omega_{a_1} = \omega_{02} - \omega_{a_2}, \tag{17}$$

we obtain the requirement

$$\Delta\omega_0 \equiv \omega_{01} - \omega_{02} = \omega_{a_1} - \omega_{a_2} = c_s(k_{a_1} - k_{a_2}). \quad (18)$$

Thus, for two laser beams of the same wavelength, i.e., $\Delta\omega_0 = 0$, it is required that $k_{a_1} = k_{a_2}$, leading to $\theta_s = 0^\circ$ or $\theta_s = 180^\circ$, while for $\Delta\omega_0 \neq 0$, the possible directions of $\mathbf{k}_s$ are determined by Eq. (18) in combination with Eqs. (3) and (4), which is much more complicated. In the following, we discuss these two cases separately.

A. SL modes for two beams with the same wavelength

For the SL modes of collective SBS, since $k_{a_1} = k_{a_2}$ when the two pump beams have the same wavelength, $\mathbf{k}_s$ is located on the bisecting plane between $\mathbf{k}_{01}$ and $\mathbf{k}_{02}$ (the xz plane in Fig. 1), and the ponderomotive response $\gamma_{\mathrm{pm}_1} = \gamma_{\mathrm{pm}_2}$ owing to the symmetric matching condition. Thus, the single-beam gain coefficient $\kappa_\alpha = (\mathrm{Im}[\gamma_{\mathrm{pm}}]k_a^2/8k_s)|a_{0\alpha}|^2\cos^2\varphi_\alpha$. Considering two beams with the same intensity, the gain coefficient for the SL mode has the upper limit $\kappa_c \le \kappa_1 + \kappa_2 \le \kappa_c^{\mathrm{U}} \equiv (\mathrm{Im}[\gamma_{\mathrm{pm}}]k_a^2/4k_s)|a_0|^2$. According to Eq. (15), $\kappa_c/\kappa_c^{\mathrm{U}}$ is the larger root of the following equation:

$$\left(\frac{2\kappa_c}{\kappa_c^{\mathrm{U}}}\right)^2 - 2(\cos^2\varphi_1 + \cos^2\varphi_2)\frac{\kappa_c}{\kappa_c^{\mathrm{U}}} + (\cos\varphi_1\cos\varphi_2\sin\delta_\perp)^2 = 0, \quad (19)$$

where the factors $\cos\varphi_1$, $\cos\varphi_2$ and $\sin\delta_\perp$ depend solely on the geometry (θ_h, φ_s, $\theta_s = 0^\circ$ or 180°) of the SL mode and the polarization states of the laser beams, which are denoted by the polarization angle β_α ($-90^\circ < \beta_\alpha \le 90^\circ$), as shown in Fig. 1. Therefore, $\kappa_c/\kappa_c^{\mathrm{U}}$ is determined completely by the beam crossing angle θ_h, the out-of-plane angle φ_s, and the polarization angles β_1 and β_2, while the dependence of κ_c^{U} on the scattered wavelength is reflected in the gain spectrum of κ_c^{U}.

For a typical plasma condition at the laser entrance hole of a He plasma,[36] κ_c^{U} is shown in Fig. 2, in which the gain coefficient is normalized by $I_{15} = I_{01}[\mathrm{W/cm^2}]/10^{15}$. For $\theta_s = 0^\circ$ and $-90^\circ < \varphi_s < 90^\circ$, where $\mathbf{k}_s$ is in the quadrants $x > 0$, the scattered wavelength increases with increasing θ_h, while the peak value of κ_c^{U} decreases with increasing θ_h. This is because the term $k_a^2\mathrm{Im}[\gamma_{\mathrm{pm}}]$ in κ_c^{U} peaks at $\omega_a \approx k_a c_s$ ($\lambda_B - \lambda_0 \propto \omega_a \propto k_a$), with its peak value decreasing with increasing k_a,[30] and $k_a = 2k_0\sin[\arccos(\cos\varphi_s\cos\theta_h)/2]$ for $\theta_s = 0^\circ$ [obtained from Eqs. (3) and (4)] increases with increasing θ_h. For $\theta_s = 180^\circ$ and $-90^\circ < \varphi_s < 90^\circ$, where $\mathbf{k}_s$ is in the quadrants $x < 0$, the scattered wavelength decreases with increasing θ_h, while the peak value of κ_c^{U} increases with increasing θ_h. This is because $k_a = 2k_0\cos[\arccos(\cos\varphi_s\cos\theta_h)/2]$ for $\theta_s = 180^\circ$ decreases with increasing θ_h. Besides, k_a increases as the angle between $\mathbf{k}_s$ and $\hat{x}$ increases from zero to 180°, which corresponds to φ_s varying from 0 to 90° for $\theta_s = 0^\circ$ and then from 90° to 0 for $\theta_s = 180^\circ$, as shown in Fig. 1. Consequently, the scattered

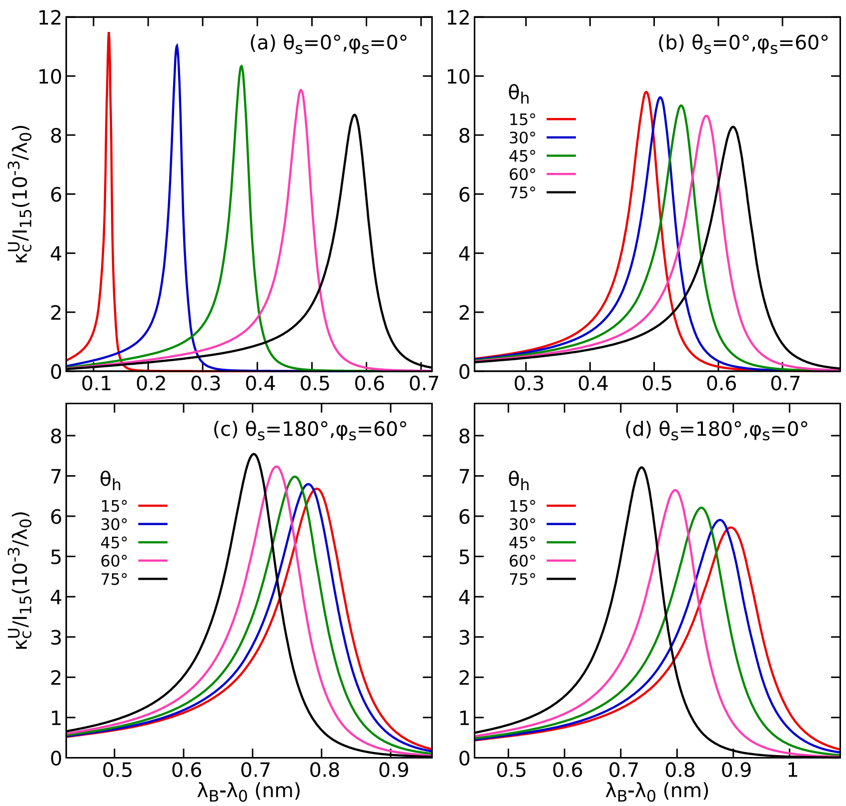

FIG. 2. $\kappa_c^{\mathrm{U}}/I_{15}$ vs $\lambda_B - \lambda_0$ for SL modes of two overlapping beams with the same intensity ($I_{01} = I_{02}$ and $I_{15} \equiv I_{01}/10^{15}$ W/cm^2) and the same vacuum wavelength ($\lambda_0 = 351$ nm) at different crossing angles for (a) $\theta_s = 0^\circ$, $\varphi_s = 0^\circ$, (b) $\theta_s = 0^\circ$, $\varphi_s = 60^\circ$, (c) $\theta_s = 180^\circ$, $\varphi_s = 60^\circ$, and (d) $\theta_s = 180^\circ$, $\varphi_s = 0^\circ$. The plasma condition $n_e = 0.06\,n_c$, $T_e = 2.8$ keV, $T_e/T_i = 3.5$, and zero flow velocity in a He plasma is taken.

wavelength increases while the peak gain value decreases as the angle between $\mathbf{k}_s$ and $\hat{x}$ increases from 0° through 90° to 180°, as shown in Fig. 2.

The influence of polarization on κ_c of the SL modes can be evaluated through κ_c/κ_c^U determined by Eq. (19). Owing to the symmetric relation $\kappa_c/\kappa_c^U|_{\theta_s=180°,\varphi_s} = \kappa_c/\kappa_c^U|_{\theta_s=0,-\varphi_s}$, in the following discussion of the modification of κ_c by polarization states, we assume $\theta_s = 0$. First, it is observed that the range of κ_c/κ_c^U attainable by adjusting the polarization angles β_1 and β_2 depends on the out-of-plane angle φ_s. In particular, $\kappa_c/\kappa_c^U = 1$ can be attained only for in-plane scattering ($\varphi_s = 0$) when both beams are s-polarized ($\beta_1 = \beta_2 = 0$), while $\kappa_c/\kappa_c^U < 1$ for all combinations of β_1 and β_2 when $\varphi_s \neq 0$. The upper and lower bounds of the range of κ_c/κ_c^U at each φ_s can be obtained analytically, as given by Eqs. (A1)–(A4) in Appendix A. Figure 3 shows the variation of the range of κ_c/κ_c^U with φ_s for different crossing angles. As can be seen, the range of variation of κ_c/κ_c^U is quite broad, especially for large obtuse crossing angles, indicating the significant role played by the polarization in the SL modes. As a result, the SL mode at some out-of-plane angle φ_s can be enhanced or reduced effectively by adjusting β_1 and β_2. For a specified φ_s, the upper bound of κ_c/κ_c^U depends on the best achievable alignment between the polarization directions of the two laser beams and the common scattered wave. Complete alignment among these three waves is only possible for in-plane scattering ($\varphi_s = 0$), where the polarization direction perpendicular to $\mathbf{k}_{01}$ and $\mathbf{k}_{02}$ is also orthogonal to $\mathbf{k}_s$. For out-of-plane scattering, the best achievable polarization alignment decreases with increasing out-of-plane angle, making κ_c/κ_c^U drop with φ_s. Notice that for an acute crossing angle where $\theta_h < 45°$, at small φ_s, for the best achievable polarization alignment, the SL modes with $\boldsymbol{a}_s$ along the direction of $\hat{y}\times\mathbf{n}_s$ have larger gain coefficient, while at large φ_s, the SL modes with $\boldsymbol{a}_s$ along the direction of $\hat{y}$ have larger gain coefficient, and the best alignment occurs when both laser beams are p-polarized, and their alignment with $\boldsymbol{a}_s$ along $\hat{y}$ is independent of φ_s, leading to a constant κ_c/κ_c^U. This results in a curvature inflection of the upper bound of κ_c/κ_c^U, as shown in Fig. 3.

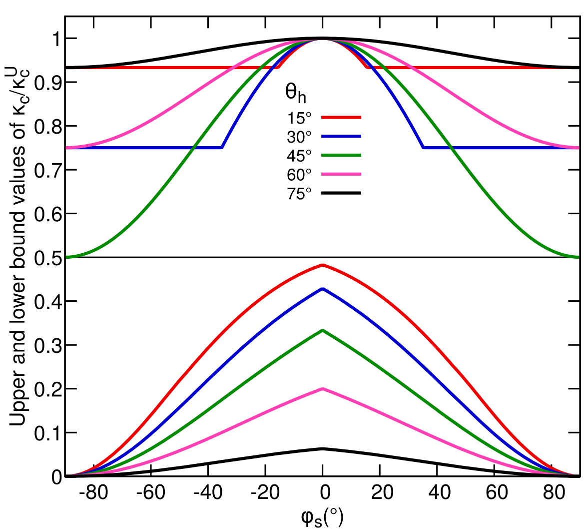

FIG. 3. Upper and lower bounds of κ_c/κ_c^U when β_1 and β_2 are varied at each out-of-plane angle φ_s. Two crossing laser beams with the same wavelength are assumed.

To see the relative importance of SL modes with different out-of-plane angles for specified polarization states, we consider the relation between κ_c/κ_c^U and φ_s when β_1 and β_2 are specified. Several special cases can be identified:

(a) When both beams I and II are s-polarized ($\beta_1 = \beta_2 = 0$), it is found that $\kappa_c/\kappa_c^U = \cos^2\varphi_s$. Consequently, for this polarization state, the in-plane SL mode is favored.

(b) When both beams are p-polarized ($\beta_1 = \beta_2 = 90°$), it is found for $|\sin\varphi_s| \le 1/\tan\theta_h$ that $\kappa_c/\kappa_c^U \equiv \cos^2\theta_h$ over $-90° < \varphi_s \le 90°$, where $\boldsymbol{a}_s$ is along the $\hat{y}$ direction, and hence its alignment with the p-polarized laser beams is independent of the out-of-plane angle; otherwise, the orthogonal mode with $\boldsymbol{a}_s$ along the $\hat{y}\times\mathbf{n}_s$ direction has a larger gain coefficient, rendering $\kappa_c/\kappa_c^U = \sin^2\theta_h\sin^2\varphi_s$, more favorable for out-of-plane modes.

(c) When the polarization directions of the two pump beams are orthogonal ($\mathbf{e}_{01}\cdot\mathbf{e}_{02} = 0$), it is found that $\boldsymbol{a}_s$ lies in the ($\mathbf{e}_{01}$, $\mathbf{e}_{02}$) plane, and the orthogonal drives of the two beams complement each other, making $\kappa_c/\kappa_c^U \equiv 1/2$ over $-90° < \varphi_s \le 90°$. Thus, κ_c is just the same as the gain coefficient of the single-beam side-scatter at the same scattering angle, for which the mode with $\mathbf{k}_s$ perpendicular to $\mathbf{e}_{0\alpha}$, and hence complete polarization alignment, is always allowed. The gain enhancement by sharing of the scattered wave vanishes for this polarization state, indicating that the SL mode can be effectively suppressed by tuning the polarization directions of the two pump beams to be orthogonal.

For other combinations of β_1 and β_2, the typical variation of κ_c/κ_c^U with φ_s is shown in Fig. 4. Generally, there exists one most favored mode corresponding to the maximum value of κ_c/κ_c^U at some out-of-plane angle φ_s^M. Further analysis shows that this maximum value is completely determined by the polarization alignment between the two pump beams,

$$\max_{\varphi_s}\left[\frac{\kappa_c}{\kappa_c^U}\right] = \frac{1}{2}\left(1 + |\cos\delta_{pol}|\right), \tag{20}$$

where

$$\begin{aligned}\cos\delta_{pol} &\equiv \mathbf{e}_{01}\cdot\mathbf{e}_{02}\\ &= \cos^2\theta_h\cos(\beta_1-\beta_2) + \sin^2\theta_h\cos(\beta_1+\beta_2).\end{aligned} \tag{21}$$

The detailed derivation is given in Appendix B. This maximum value is attained when the polarization direction of $\boldsymbol{a}_s$ is along the bisector of the acute angles between $\mathbf{e}_{01}$ and $\mathbf{e}_{02}$ (i.e., along $\mathbf{e}_{01} + \mathbf{e}_{02}$ for $\cos\delta_{pol} > 0$ and $\mathbf{e}_{01} - \mathbf{e}_{02}$ for $\cos\delta_{pol} < 0$). This condition, together with the requirement $\boldsymbol{a}_s \perp \mathbf{k}_s$, then gives

$$\tan\varphi_s^M = \begin{cases} -\tan[(\beta_1-\beta_2)/2]\sin\theta_h, & \cos\delta_{pol} > 0,\\ \dfrac{\sin\theta_h}{\tan[(\beta_1-\beta_2)/2]}, & \cos\delta_{pol} < 0.\end{cases} \tag{22}$$

Therefore, the out-of-plane angle $|\varphi_s^M|$ of the most favored SL mode is largely determined by $\beta_1 - \beta_2$, which characterizes the overall deviation from s-polarization of beams I and II. Typically, there is a jump in φ_s^M at $\cos\delta_{pol} = 0$, where the sign of φ_s^M becomes opposite. Before this jump, $|\varphi_s^M|$ increases with increasing $|\beta_1 - \beta_2|$, and after it, $|\varphi_s^M|$ decreases with increasing $|\beta_1 - \beta_2|$. For an acute crossing angle with $\theta_h < 45°$, the upper limit of $|\varphi_s^M|$ is $\arctan(\sin\theta_h/\sqrt{\cos 2\theta_h})$, corresponding to 15.5° and 35.3° for $\theta_h = 15°$ and 30°, respectively,

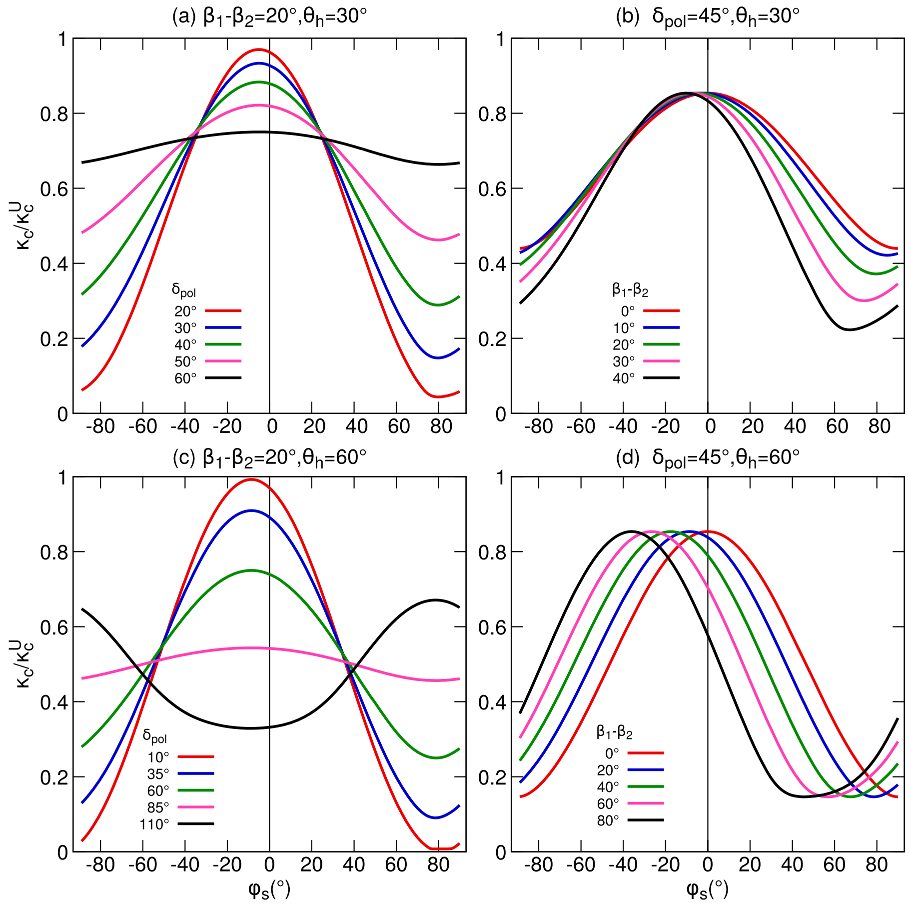

FIG. 4. κ_c/κ_c^U vs φ_s for SL modes of two beams with (a) and (b) $\theta_h = 30^\circ$ and (c) and (d) $\theta_h = 60^\circ$.

while for an obtuse crossing angle with $\theta_h > 45^\circ$, $|\varphi_s^M|$ can reach 90° when $\beta_1 = \beta_2 \geq 90^\circ - \arccos(1/\tan^2\theta_h)/2$. Thus, for small acute crossing angles, the out-of-plane modes with relatively small out-of-plane angles can be favored for some polarization states, while for large obtuse crossing angles, the large-angle out-of-plane SL modes can also be favored.

In practice, the overlapping volume of the laser beam is finite, limiting the amplification length l_{amp} (along the $\mathbf{n}_s$ direction) of the SL modes. If it is assumed that the laser width is w_b, then, to enclose the amplification length inside the overlapping volume, it is required that $l_{amp}|\mathbf{n}_{s\perp\mathbf{k}_{01}}| \leq w_b$ and $l_{amp}|\mathbf{n}_{s\perp\mathbf{k}_{02}}| \leq w_b$, where $\mathbf{n}_{s\perp\mathbf{k}_{0\alpha}}$ is the projection of $\mathbf{n}_s$ onto the plane perpendicular to the laser propagation direction $\mathbf{k}_{0\alpha}$. This gives the greatest amplification length $l_{amp} = w_b/\sqrt{1-\cos^2\varphi_s\cos^2\theta_h}$ for two beams at the same wavelength. It can be seen that l_{amp} decreases with increasing out-of-plane angle; however, the rate of decrease drops with increasing crossing angle, corresponding to a decrease of about 74%, 50%, 29%, 13%, and 3% when φ_s increases from 0° to 90°, for θ_h at 15°, 30°, 45°, 60° and 75°, respectively. Considering this effect, the achievable gain $\kappa_c l_{amp}/w_b$ of the SL modes with different out-of-plane angles is shown in Fig. 5 for three polarization combinations $\beta_1 = \beta_2 = 0$, $\beta_1 = -\beta_2 = 45^\circ$, and $\beta_1 = \beta_2 = 90^\circ$, where the value of κ_c at the peak wavelength is used. For small crossing angle $\theta_h = 15^\circ$, the gains of the in-plane modes are always larger than those of the out-of-plane modes, irrespective of the beam polarization, owing to the rapidly falling amplification length with increasing φ_s. For larger crossing angles, however, the relative importance of the out-of-plane modes with respect to the in-plane modes depends on the polarization states of the laser beams. Especially for large obtuse crossing angles, the gains of the out-of-plane SL modes can significantly exceed those of the in-plane modes for certain polarization states, even when the effects of finite beam overlapping volume have been taken into account.

B. SL modes for two beams with nonzero wavelength difference

For two beams with nonzero wavelength difference, on substituting the expression (3) for $k_{es_1} = k_{a_1}$ and $k_{es_2} = k_{a_2}$ into the matching requirement (18) for the SL mode, it is found that

$$\frac{\Delta\omega_0}{4k_{01}c_s} = \cos\frac{\vartheta_1+\vartheta_2}{4}\sin\frac{\vartheta_1-\vartheta_2}{4}, \tag{23}$$

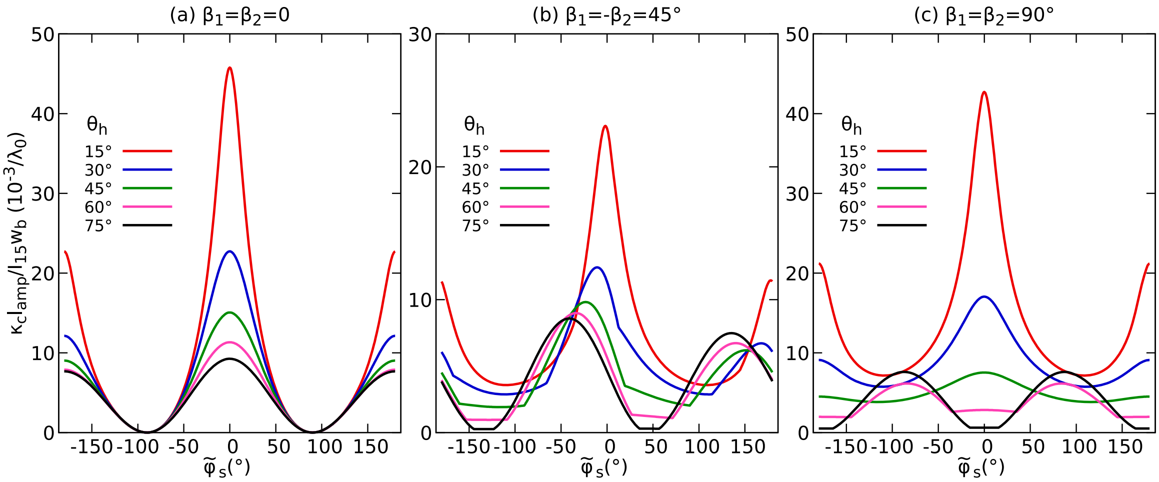

FIG. 5. Achievable $\kappa_c l_{amp}/I_{15}w_b$ vs $\tilde{\varphi}_s$ for (a) $\beta_1 = \beta_2 = 0$, (b) $\beta_1 = -\beta_2 = 45^\circ$, and (c) $\beta_1 = \beta_2 = 90^\circ$, where $\tilde{\varphi}_s$ as the angle from the bisector of $\mathbf{k}_{01}$ and $\mathbf{k}_{02}$ (x direction) to $\mathbf{n}_s$, is equal to φ_s for SL modes with $\theta_s = 0$, and is equal to $\varphi_s \pm 180^\circ$ for SL modes with $\theta_s = 180^\circ$. The condition $\lambda_0 = 351$ nm, $n_e = 0.06\, n_c$, $T_e = 2.5$ keV, $T_e/T_i = 3.5$, and zero flow velocity for He plasma is taken.

where the scattering angles ϑ_1 for beam I and ϑ_2 for beam II are functions of θ_h, θ_s, and φ_s. Without loss of generality, we designate the beam with shorter wavelength as beam I, and then $\Delta\omega_0 = \omega_{01} - \omega_{02} \geq 0$ and $\Delta\lambda_0 = \lambda_{02} - \lambda_{01} \approx \lambda_{01}^2 \Delta\omega_0/2\pi c \geq 0$, where λ_{01} and λ_{02} are the vacuum wavelengths of beams I and II, respectively. Since the maximum value of the right-hand side of Eq. (23) as a function of θ_s and φ_s is $\frac{1}{2}\sin\theta_h$ located at $\theta_s = \theta_h$ and $\varphi_s = 0$, it is required that $\Delta\omega_0 \leq 2k_{01}c_s \sin\theta_h$ and hence $\Delta\lambda_0 \leq 2\lambda_{01}c_s \sin\theta_h \sqrt{1 - n_e/n_c}/c$ for the SL modes to exist. For given $\Delta\lambda_0$, the possible directions of $\mathbf{k}_s$ for the SL modes as obtained from Eq. (23) constitute a loop on the (θ_s, φ_s) sphere, as shown in Fig. 6. When $\Delta\lambda_0 = 0$, the $\mathbf{k}_s$ loop constitutes a great circle in the xz plane perpendicular to $\mathbf{k}_{01} - \mathbf{k}_{02}$. With increasing $\Delta\lambda_0$, the $\mathbf{k}_s$ loop contracts to a smaller and smaller loop encircling the wavevector direction of the laser beam with longer wavelength (here the direction of $\mathbf{k}_{02}$ at $\theta_s = \theta_h$ and $\varphi_s = 0$), until at the greatest allowed wavelength difference $2\lambda_{01}c_s \sin\theta_h \sqrt{1 - n_e/n_c}/c$, the $\mathbf{k}_s$ loop retracts to one point corresponding to the direction of $\mathbf{k}_{02}$. The contraction of the $\mathbf{k}_s$ loop is more severe for a smaller beam crossing angle, for which the greatest allowed wavelength difference is smaller. By tuning the wavelength difference between the two pump beams greater than $2\lambda_{01}c_s \sqrt{1 - n_e/n_c}/c$, SL modes are diminished for any beam crossing angle. This provides an efficient way to suppress the SL modes of SBS.

The $\mathbf{k}_s$ loop can be parameterized by $-180^\circ < \alpha_\perp \leq 180^\circ$, the angle from $(\mathbf{k}_{01}, \mathbf{k}_{02})$ plane to $(\mathbf{k}_s, \mathbf{k}_{02})$ plane, where the in-plane SL modes correspond to $\alpha_\perp = 0$ or 180°.[44] One upper bound of κ_c for all possible

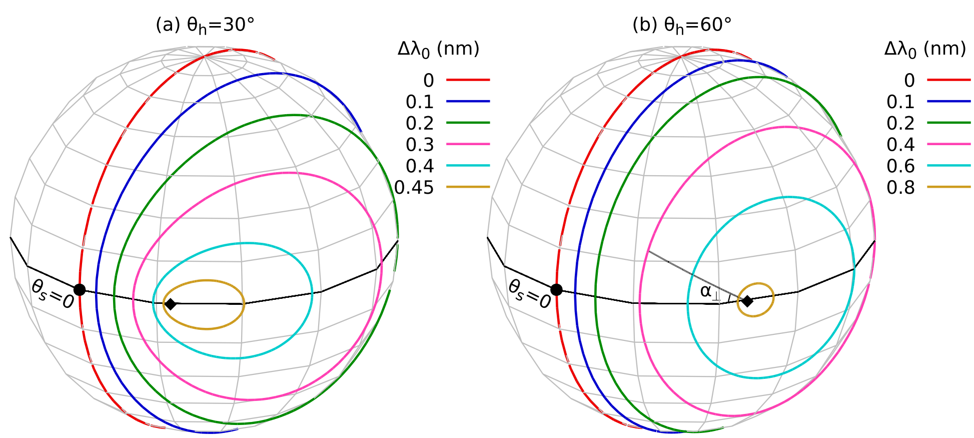

FIG. 6. Possible directions of $\mathbf{k}_s$ for SL modes of two crossing beams with different wavelength differences for beam crossing angles (a) $\theta_h = 30^\circ$ and (b) $\theta_h = 60^\circ$. The $(\mathbf{k}_{01}, \mathbf{k}_{02})$ plane corresponding to $\varphi_s = 0$ is indicated by the dashed curve, on which $\theta_s = 0$ as marked by the black circle corresponds to the bisector direction of $\mathbf{k}_{01}$ and $\mathbf{k}_{02}$, and $\theta_s = \theta_h$ as marked by the black diamond corresponds to the direction of $\mathbf{k}_{02}$. The indicated angle $\alpha_\perp$ from the $(\mathbf{k}_{01}, \mathbf{k}_{02})$ plane to the $(\mathbf{k}_s, \mathbf{k}_{02})$ plane can be used to denote different SL modes for specified $\Delta\lambda_0$ and θ_h. The example of a He plasma with conditions $\lambda_{01} = 351$ nm, $n_e = 0.06\, n_c$, $T_e = 2.8$ keV, $T_e/T_i = 3.5$, and zero flow velocity is taken.

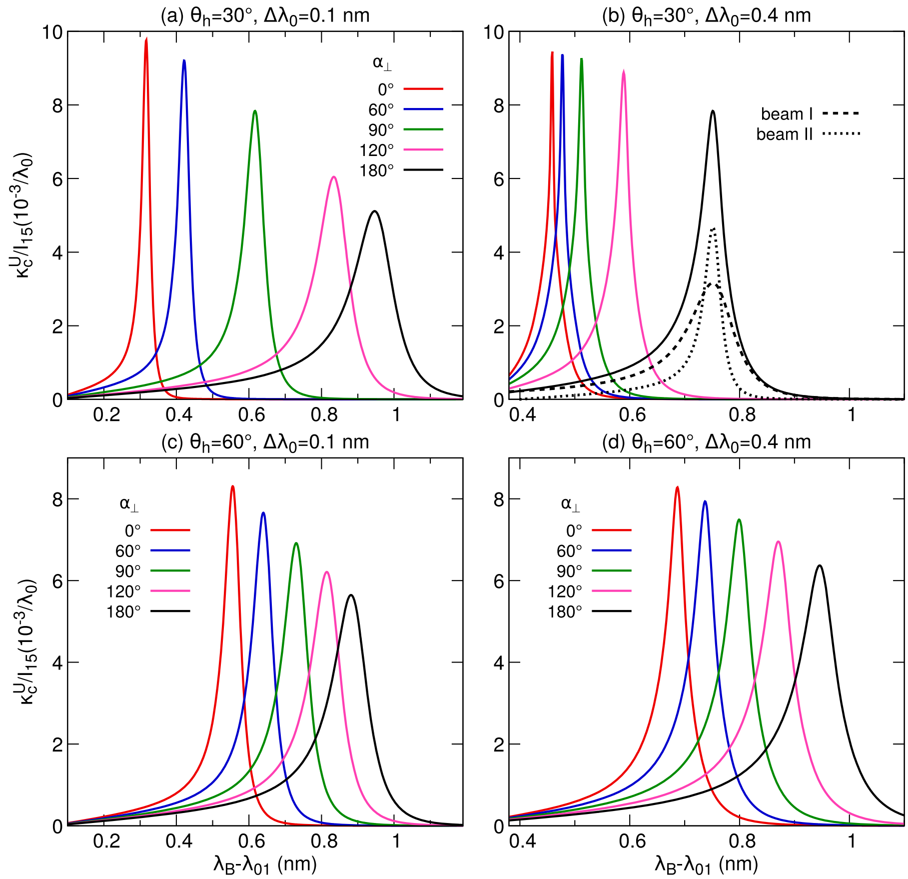

FIG. 7. κ_c^U vs $\lambda_B - \lambda_{01}$ for SL modes of two crossing beams with different wavelength differences and crossing angles. The contributions of beams I and II are shown by dashed and dotted curves, respectively, for the example of $\alpha_\perp = 180^\circ$ in (b). The example of a He plasma with conditions $\lambda_{01} = 351$ nm, $n_e = 0.06\, n_c$, $T_e = 2.8$ keV, $T_e/T_i = 3.5$, and zero flow velocity is taken.

polarization states is $\kappa_c^U = \sum_{\alpha=1,2} \mathrm{Im}[\gamma_{pm_\alpha}] k_{a_\alpha}^2 |a_{0\alpha}|^2 / 8k_s$. We can again can use κ_c^U to characterize the dependence of κ_c on the scattered wavelength, as shown in Fig. 7 for SL modes of two laser beams with different wavelength differences. Since the system is symmetric with respect to reflection at the $(\mathbf{k}_{01}, \mathbf{k}_{02})$ plane, $0 \le \alpha_\perp \le 180^\circ$ is shown. In Fig. 7(b), the contributions of beams I and II to κ_c^U are also displayed for $\alpha_\perp = 180^\circ$. Since $k_{a_2} < k_{a_1}$, the contribution of beam II has a greater peak value yet a narrower width compared with beam I. Hence, beam II with the longer wavelength contributes more to the peak of κ_c^U, whereas beam I with the shorter wavelength contributes more to the wing of κ_c^U. For each $\Delta\lambda_0$, because the scattering angles ϑ_1 and ϑ_2 and hence k_{a_1} and k_{a_2} increase with increasing $\alpha_\perp$, the peak wavelength increases with increasing $\alpha_\perp$, while the peak value of κ_c^U decreases. Furthermore, with increasing $\Delta\lambda_0$, the shortest peak wavelength of the SL mode with $\alpha_\perp = 0$ increases, while the longest peak wavelength of the SL mode with $\alpha_\perp = 180^\circ$ decreases, because of the contraction of the $\mathbf{k}_s$ loop. This leads to a narrower wavelength range for the possible SL modes when the laser wavelength difference is enlarged. Also, it can be shown that the shortest peak wavelength of the SL mode with $\alpha_\perp = 0$ increases with increasing θ_h, while the longest peak wavelength of the SL mode with $\alpha_\perp = 180^\circ$ increases with increasing θ_h when $\theta_h < 2\arcsin(\sqrt{|\Delta\omega_0|/4k_0c_s})$, and decreases with increasing θ_h for a larger beam crossing angle.

Taking into account the effects of the polarization states and the finite beam overlapping volume of the two laser beams, the achievable $\kappa_c l_{\mathrm{amp}}/w_b$ can be calculated for an arbitrary allowed $\Delta\lambda_0$, similar to the case for $\Delta\lambda_0 = 0$. Combining the results for different $\Delta\lambda_0$ and taking the value of κ_c at the peak wavelength, a map of $\kappa_c l_{\mathrm{amp}}/w_b$ vs the direction of $\mathbf{k}_s$ can be obtained, as shown in Fig. 8, where a view along the $-\hat{y}$ direction (cf. Fig. 1) is taken. It is clear that the polarization states can significantly modify the gain of the SL modes. Especially for large beam crossing angles and relatively small $\Delta\lambda_0$, for which the $\mathbf{k}_s$ loop is relatively large, the out-of-plane SL modes with φ_s deviating from zero can be quite important, similar to the case with zero laser wavelength difference discussed above.

IV. DISCUSSION AND SUMMARY

In summary, based on a linear kinetic model, an analytic convective solution has been derived for the SL modes of two overlapped laser beams. The effects of crossing angle, polarization states, and the finite overlapping volume of the two beams on the collective SBS modes with shared scattered waves have been discussed

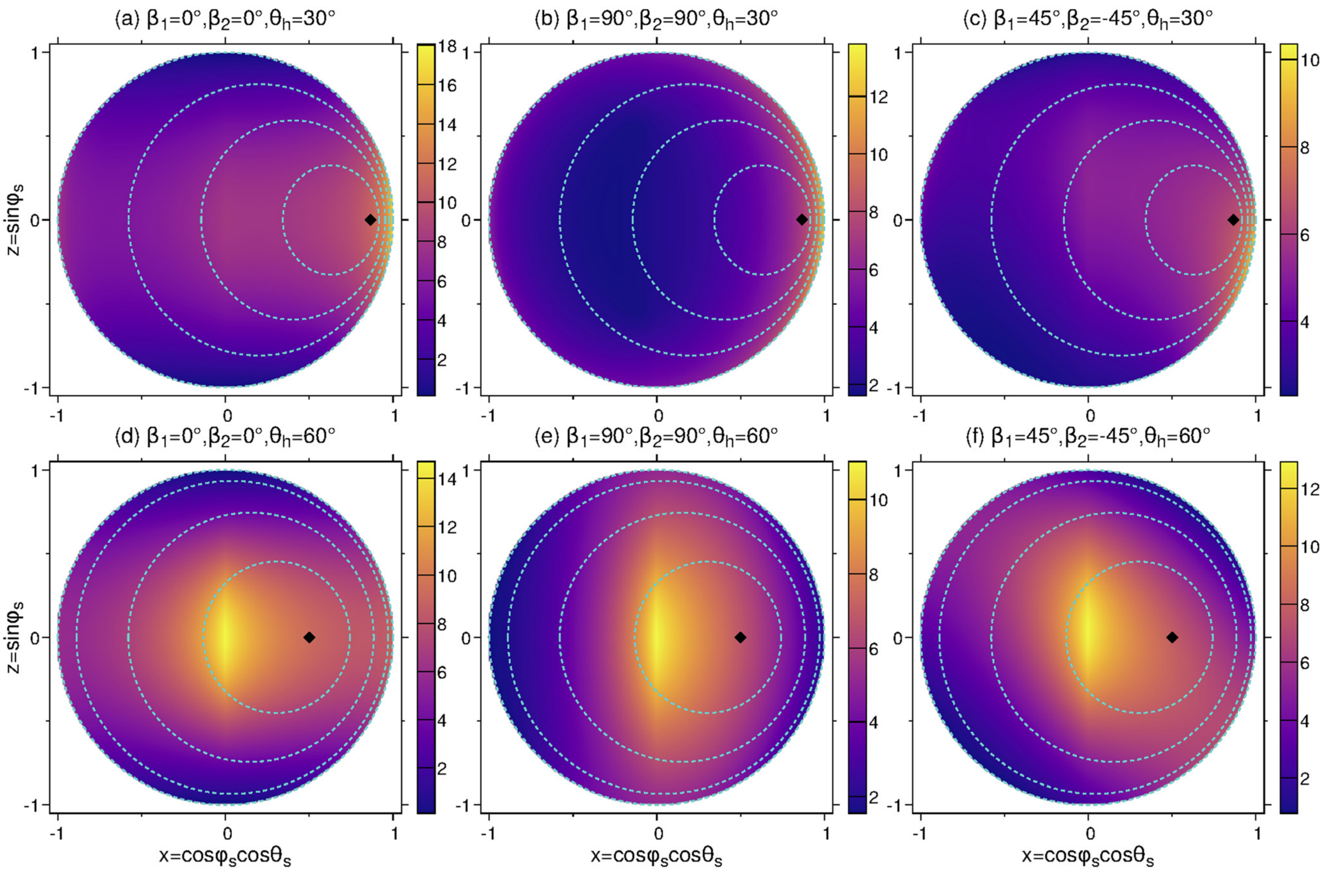

FIG. 8. Maps of $\kappa_c l_{amp}/w_b I_{15}$ vs the direction of $\mathbf{k}_s$ for SL modes of two crossing beams with different combinations of β_1 and β_2 at (a)–(c) $\theta_h = 30^\circ$ and (d)–(f) $\theta_h = 60^\circ$. The direction of view is taken along $-y$, making the $\mathbf{k}_s$ loop for $\Delta\lambda_0 = 0$ appear as a unit circle on the maps. For $\theta_h = 30^\circ$, the $\mathbf{k}_s$ loops corresponding to $\Delta\lambda_0$ equal to 0, 0.2, 0.3, and 0.4 nm, which encircle the direction of $\mathbf{k}_{02}$ (marked by the black diamonds), are shown by the cyan curves, while for $\theta_h = 60^\circ$, the $\mathbf{k}_s$ loops corresponding to $\Delta\lambda_0$ equal to 0, 0.2, 0.4, and 0.6 nm are displayed. The example of a He plasma with conditions λ_{01} = 351 nm, n_e = 0.06 n_c, T_e = 2.8 keV, T_e/T_i = 3.5, and zero flow velocity is taken.

in detail for both zero and nonzero wavelength differences between the two laser beams. When the two beams are of the same wavelength, the wavevectors of the shared scattered waves lie on a circle in the bisecting plane between the wavevectors of the two laser beams. The wavelength of the scattered waves varies with the beam crossing angle and the out-of-plane angle of the SL modes. The gain coefficients of the SL modes, on the other hand, are also subject to the polarization states of the laser beams. When the two laser beams are both s-polarized, the gain coefficient of the SL mode is twice the gain coefficient of a single beam, while when the polarization directions of the two beams are orthogonal to each other, the gain coefficient of the collective SBS modes becomes the same as the single-beam side-scatter with the same scattering angle. Furthermore, for some polarization states and especially for obtuse crossing angles, the out-of-plane SL modes can become more important than the in-plane modes. With increasing wavelength difference between the two laser beams, the possible directions of the wavevectors of the common scattered wave contract toward the wavevector direction of the pump beam with longer wavelength. This changes the scattered wavelengths and the gain coefficients of the SL modes. Nevertheless, depending on the polarization state and the beam crossing angle, the out-of-plane modes can still be quite important. Finally, for sufficiently large vacuum wavelength difference $\Delta\lambda_0 > 2\lambda_{01} c_s \sqrt{1 - n_e/n_c}/c$, the SL modes of SBS no longer exist, which provides an efficient way to suppress the SL modes of SBS.

In this work, uniform plasma conditions with zero flow velocity have been assumed for an illustrative analysis. A nonzero flow velocity effectively leads to an additional wavelength difference between the two laser beams, which can also be accounted for by our model. Furthermore, in ICF, various laser smoothing techniques, such as kinoform/random phase plate (KPP/RPP),[37] smoothing by spectral dispersion (SSD),[38] polarization smoothing (PS),[39] and some new methods,[40–42] are often used to suppress LPI. Consequently, the laser beam intensity distribution can be highly nonuniform with many high-intensity speckles, and the induced temporal/spatial incoherence of the laser beam introduces additional mismatching into SBS, leading to a modified ponderomotive response γ_{pm}.[43] To obtain a precise gain by integrating the local gain coefficient, these two factors, along with the realistic overlapping pattern of the laser beams,[20,32] should be properly taken into account in further simulations. The collective SL modes can have much higher gain coefficient than single-beam SBS, and consequently they can be amplified to a great magnitude over a short distance. Especially for practical inhomogeneous plasmas, when the resonance length is limited by the inhomogeneity of the flow velocity or temperature,[5,32] the collective SL mode could dominate over the single-beam SBS mode. Finally, from a comparison with the collective SP modes investigated in Ref. 30, it is found that depending on the crossing angle, polarization states, and the wavelength difference between the two laser beams, either the SP or the SL mode can be more important. Simulations under realistic plasma and laser conditions are required to assess the importance of the SL modes, for which this work provides valuable theoretical references.

ACKNOWLEDGMENTS

This work was supported by the National Key R&D Program of China (Grant No. 2017YFA0403204), the Science Challenge Project (Grant No. TZ2016005), the National Natural Science Foundation of China (Grant Nos. 11 875 093 and 11 875 091), and the Project supported by CAEP Foundation (Grant No. CX20210040).

APPENDIX A: ACHIEVABLE RANGE OF κ_c/κ_c^U AT EACH φ_s BY ADJUSTING β_1 AND β_2 FOR TWO CROSSING BEAMS WITH SAME WAVELENGTH AND INTENSITY

By analysis, it is found that both the upper and lower bounds of κ_c/κ_c^U are attained at $\beta_1 = -\beta_2$, when the polarization states of beams I and II are symmetric with respect to the bisecting plane between $\mathbf{k}_{01}$ and $\mathbf{k}_{02}$. The upper bound is

$$\max_{\beta_{1,2}}\left[\frac{\kappa_c}{\kappa_c^U}\right] = \max\left[1 - \cos^2\theta_h \sin^2\varphi_s, \cos^2\theta_h\right], \tag{A1}$$

and the corresponding polarization angles are

$$\beta_1 = -\beta_2 = \begin{cases} -\arctan(\tan\varphi_s \sin\theta_h), & |\sin\varphi_s| < \tan\theta_h, \\ \pm 90^\circ, & \text{otherwise.} \end{cases} \tag{A2}$$

For the former case, $\boldsymbol{a}_s$ is along the direction of $\hat{y} \times \mathbf{n}_s$, and for the latter case, $\boldsymbol{a}_s$ is along the direction of $\hat{y}$. The lower bound is

$$\min_{\beta_{1,2}}\left[\frac{\kappa_c}{\kappa_c^U}\right] = \frac{(\cos\varphi_s \cos\theta_h)^2}{\cos^2\varphi_s + (\cos\theta_h + \sin\theta_h|\sin\varphi_s|)^2} \tag{A3}$$

and the corresponding polarization angles are

$$\beta_1 = -\beta_2 = \arctan\left(\frac{\mathrm{sgn}(\varphi_s)\cos\varphi_s}{\cos\theta_h + \sin\theta_h|\sin\varphi_s|}\right), \tag{A4}$$

where sgn(·) is the sign function.

APPENDIX B: MAXIMUM VALUE OF κ_c/κ_c^U VS φ_s FOR TWO CROSSING BEAMS WITH SAME WAVELENGTH AND INTENSITY WHEN THEIR POLARIZATION STATES ARE GIVEN

In this case, the polarization direction of beam α ($\alpha = 1, 2$) along the unit vector $\mathbf{e}_{0\alpha}$ is given while the propagation direction $\mathbf{n}_s$ of the scattered light is varied. To obtain $\max_{\varphi_s}[\kappa_c/\kappa_c^U]$, it is much easier to express φ_1, φ_2 and $\delta_\perp$ in Eq. (19) in terms of the relative orientation between $\mathbf{e}_{01}$, $\mathbf{e}_{02}$, and $\mathbf{n}_s$. Without loss of generality, for now we assume the angle δ_{pol} between $\mathbf{e}_{01}$ and $\mathbf{e}_{02}$ is less than 90°, making $\cos\delta_{\mathrm{pol}} \geq 0$. (Since the unit polarization vectors can be chosen freely between $\pm\mathbf{e}_{01}$ and $\pm\mathbf{e}_{02}$, we can always ensure an acute angle between them.) Denoting the angle between $\mathbf{n}_s$ and the ($\mathbf{e}_{01}$, $\mathbf{e}_{02}$) plane as $\theta_\perp$, and the angle between the projection of $\mathbf{n}_s$ onto this plane and the bisector of $\mathbf{e}_{01}$ and $\mathbf{e}_{02}$ as $\theta_\parallel$, we have $\sin\varphi_\alpha = \mathbf{e}_{0\alpha}\cdot\mathbf{n}_s = \cos\theta_\perp\cos(\theta_\parallel \pm \delta_{\mathrm{pol}}/2)$ ($\alpha = 1, 2$), and $\sin\delta_\perp \cos\varphi_1 \cos\varphi_2 = (\mathbf{e}_{01} \times \mathbf{e}_{02})\cdot\mathbf{n}_s = \sin\delta_{\mathrm{pol}}\sin\theta_\perp$. [See Eq. (12).] Equation (19) can thus be written as

$$\left(\frac{2\kappa_c}{\kappa_c^U}\right)^2 - \left[2 - \cos^2\theta_\perp(1 + \cos 2\theta_\parallel \cos\delta_{\mathrm{pol}})\right]\frac{2\kappa_c}{\kappa_c^U} + \sin^2\delta_{\mathrm{pol}}\sin^2\theta_\perp = 0. \tag{B1}$$

With the change in the direction of $\mathbf{n}_s$, both $\theta_\parallel$ and $\theta_\perp$ change, and it is easy to see that the larger root of this quadratic equation increases with decreasing $\cos 2\theta_\parallel$, and so $\max_{\theta_\parallel}[\kappa_c/\kappa_c^U]$ is attained when $\cos 2\theta_\parallel = -1$. At $\cos 2\theta_\parallel = -1$, Eq. (B1) becomes

$$\left(\frac{2\kappa_c}{\kappa_c^U}\right)^2 - \left[1 + \cos\delta_{\mathrm{pol}} + \sin^2\theta_\perp(1 - \cos\delta_{\mathrm{pol}})\right]\frac{2\kappa_c}{\kappa_c^U} + \sin^2\delta_{\mathrm{pol}}\sin^2\theta_\perp = 0. \tag{B2}$$

Since $\cos\delta_{\mathrm{pol}} \geq 0$ is assumed, it can be determined that the larger root for κ_c/κ_c^U is $(1 + \cos\delta_{\mathrm{pol}})/2$. Since this maximum value is independent of $\theta_\perp$, we have actually obtained $\max_{\theta_\parallel,\theta_\perp}[\kappa_c/\kappa_c^U] = \max_{\varphi_s}[\kappa_c/\kappa_c^U] = (1 + |\cos\delta_{\mathrm{pol}}|)/2$. Furthermore, from Eq. (16), it can be found that for this maximum value, $\boldsymbol{a}_s$ is along $\mathbf{e}_{01} + \mathbf{e}_{02}$, i.e., the bisector of acute angles between $\mathbf{e}_{01}$ and $\mathbf{e}_{02}$.

REFERENCES

[1] J. F. Myatt, J. Zhang, R. W. Short, A. V. Maximov, W. Seka, D. H. Froula, D. H. Edgell, D. T. Michel, I. V. Igumenshchev, D. E. Hinkel, P. Michel, and J. D. Moody, "Multiple-beam laser-plasma interactions in inertial confinement fusion," Phys. Plasmas **21**, 055501 (2014).

[2] R. K. Kirkwood, J. D. Moody, J. Kline, E. Dewald, S. Glenzer, L. Divol, P. Michel, D. Hinkel, R. Berger, E. Williams, J. Milovich, L. Yin, H. Rose, B. Macgowan, O. Landen, M. Rosen, and J. Lindl, "A review of laser-plasma interaction physics of indirect-drive fusion," Plasma Phys. Controlled Fusion **55**, 103001 (2013).

[3] V. Tikhonchuk, Y. J. Gu, O. Klimo, J. Limpouch, and S. Weber, "Studies of laser-plasma interaction physics with low-density targets for direct-drive inertial confinement schemes," Matter Radiat. Extremes **4**, 045402 (2019).

[4] P. Michel, L. Divol, E. A. Williams, S. Weber, C. A. Thomas, D. A. Callahan, S. W. Haan, J. D. Salmonson, S. Dixit, D. E. Hinkel, M. J. Edwards, B. J. MacGowan, J. D. Lindl, S. H. Glenzer, and L. J. Suter, "Tuning the implosion symmetry of ICF targets via controlled crossed-beam energy transfer," Phys. Rev. Lett. **102**, 025004 (2009).

[5] P. Michel, S. H. Glenzer, L. Divol, D. K. Bradley, D. Callahan, S. Dixit, S. Glenn, D. Hinkel, R. K. Kirkwood, J. L. Kline, W. L. Kruer, G. A. Kyrala, S. Le Pape, N. B. Meezan, R. Town, K. Widmann, E. A. Williams, B. J. MacGowan, J. Lindl, and L. J. Suter, "Symmetry tuning via controlled crossed-beam energy transfer on the National Ignition Facility," Phys. Plasmas **17**, 056305 (2010).

[6] J. D. Moody, P. Michel, L. Divol, R. L. Berger, E. Bond, D. K. Bradley, D. A. Callahan, E. L. Dewald, S. Dixit, M. J. Edwards, S. Glenn, A. Hamza, C. Haynam, D. E. Hinkel, N. Izumi, O. Jones, J. D. Kilkenny, R. K. Kirkwood, J. L. Kline, W. L. Kruer, G. A. Kyrala, O. L. Landen, S. LePape, J. D. Lindl, B. J. MacGowan, N. B. Meezan, A. Nikroo, M. D. Rosen, M. B. Schneider, D. J. Strozzi, L. J. Suter, C. A. Thomas, R. P. J. Town, K. Widmann, E. A. Williams, L. J. Atherton, S. H. Glenzer, and E. I. Moses, "Multistep redirection by cross-beam power transfer of ultrahigh-power lasers in a plasma," Nat. Phys. **8**, 344–349 (2012).

[7] L. Hao, X. Y. Hu, C. Y. Zheng, B. Li, J. Xiang, and Z. J. Liu, "Study of crossed-beam energy transfer process with large crossing angle in three-dimension," Laser Part. Beams **34**, 270–275 (2016).

[8] V. V. Eliseev, W. Rozmus, V. T. Tikhonchuk, and C. E. Capjack, "Interaction of crossed laser beams with plasmas," Phys. Plasmas **3**, 2215–2217 (1996).

[9]D. Turnbull, P. Michel, J. E. Ralph, L. Divol, J. S. Ross, L. F. Berzak Hopkins, A. L. Kritcher, D. E. Hinkel, and J. D. Moody, "Multibeam seeded Brillouin sidescatter in inertial confinement fusion experiments," Phys. Rev. Lett. **114**, 125001 (2015).
[10]D. T. Michel, A. V. Maximov, R. W. Short, S. X. Hu, J. F. Myatt, W. Seka, A. A. Solodov, B. Yaakobi, and D. H. Froula, "Experimental validation of the two-plasmon-decay common-wave process," Phys. Rev. Lett. **109**, 155007 (2012).
[11]P. Michel, L. Divol, E. L. Dewald, J. L. Milovich, M. Hohenberger, O. S. Jones, L. B. Hopkins, R. L. Berger, W. L. Kruer, and J. D. Moody, "Multibeam stimulated Raman scattering in inertial confinement fusion conditions," Phys. Rev. Lett. **115**, 055003 (2015).
[12]J. D. Lindl, P. Amendt, R. L. Berger, S. G. Glendinning, S. H. Glenzer, S. W. Haan, R. L. Kauffman, O. L. Landen, and L. J. Suter, "The physics basis for ignition using indirect-drive targets on the National Ignition Facility," Phys. Plasmas **11**, 339–491 (2004).
[13]D. S. Montgomery, "Two decades of progress in understanding and control of laser plasma instabilities in indirect drive inertial fusion," Phys. Plasmas **23**, 055601 (2016).
[14]Q. S. Feng, Z. J. Liu, L. H. Cao, C. Z. Xiao, L. Hao, C. Y. Zheng, C. Ning, and X. T. He, "Interaction of parametric instabilities from 3ω and 2ω lasers in large-scale inhomogeneous plasmas," Nucl. Fusion **60**, 066012 (2020).
[15]Q. S. Feng, L. H. Cao, Z. J. Liu, C. Y. Zheng, and X. T. He, "Stimulated Brillouin scattering of backward stimulated Raman scattering," Sci. Rep. **10**, 3492 (2020).
[16]L. Hao, W. Y. Huo, Z. J. Liu, J. Li, C. Y. Zheng, and C. Ren, "A frequency filter of backscattered light of stimulated Raman scattering due to the Raman rescattering in the gas-filled hohlraums," Nucl. Fusion **61**, 036041 (2021).
[17]Y. Ji, C. W. Lian, R. Yan, C. Ren, D. Yang, Z. H. Wan, B. Zhao, C. Wang, Z. H. Fang, and J. Zheng, "Convective amplification of stimulated Raman rescattering in a picosecond laser plasma interaction regime," Matter Radiat. Extremes **6**, 015901 (2021).
[18]R. K. Kirkwood, P. Michel, R. London, J. D. Moody, E. Dewald, L. Yin, J. Kline, D. Hinkel, D. Callahan, N. Meezan, E. Williams, L. Divol, B. L. Albright, K. J. Bowers, E. Bond, H. Rose, Y. Ping, T. L. Wang, C. Joshi, W. Seka, N. J. Fisch, D. Turnbull, S. Suckewer, J. S. Wurtele, S. Glenzer, L. Suter, C. Haynam, O. Landen, and B. J. Macgowan, "Multi-beam effects on backscatter and its saturation in experiments with conditions relevant to ignition," Phys. Plasmas **18**, 056311 (2011).
[19]C. Neuville, V. Tassin, D. Pesme, M.-C. Monteil, P.-E. Masson-Laborde, C. Baccou, P. Fremerye, F. Philippe, P. Seytor, D. Teychenné, W. Seka, J. Katz, R. Bahr, and S. Depierreux, "Experimental evidence of the collective Brillouin scattering of multiple laser beams sharing acoustic waves," Phys. Rev. Lett. **116**, 235002 (2016).
[20]S. Depierreux, C. Neuville, V. Tassin, M.-C. Monteil, P.-E. Masson-Laborde, C. Baccou, P. Fremerye, F. Philippe, P. Seytor, D. Teychenné, J. Katz, R. Bahr, M. Casanova, N. Borisenko, L. Borisenko, A. Orekhov, A. Colaitis, A. Debayle, G. Duchateau, A. Heron, S. Huller, P. Loiseau, P. Nicolai, C. Riconda, G. Tran, C. Stoeckl, W. Seka, V. Tikhonchuk, D. Pesme, and C. Labaune, "Experimental investigation of the collective stimulated Brillouin and Raman scattering of multiple laser beams in inertial confinement fusion experiments," Plasma Phys. Controlled Fusion **62**, 014024 (2019).
[21]W. Seka, H. A. Baldis, J. Fuchs, S. P. Regan, D. D. Meyerhofer, C. Stoeckl, B. Yaakobi, R. S. Craxton, and R. W. Short, "Multibeam stimulated Brillouin scattering from hot, solid-target plasmas," Phys. Rev. Lett. **89**, 175002 (2002).
[22]T. Gong, L. Hao, Z. C. Li, D. Yang, S. W. Li, X. Li, L. Guo, S. Y. Zou, Y. Y. Liu, X. H. Jiang, X. S. Peng, T. Xu, X. M. Liu, Y. L. Li, C. Y. Zheng, H. B. Cai, Z. J. Liu, J. Zheng, Z. B. Wang, Q. Li, P. Li, R. Zhang, Y. Zhang, F. Wang, D. Wang, F. Wang, S. Y. Liu, J. M. Yang, S. E. Jiang, B. H. Zhang, and Y. K. Ding, "Recent research progress of laser plasma interactions in Shenguang laser facilities," Matter Radiat. Extremes **4**, 055202 (2019).
[23]D. F. DuBois, B. Bezzerides, and H. A. Rose, "Collective parametric instabilities of many overlapping laser beams with finite bandwidth," Phys. Fluids B **4**, 241–251 (1992).
[24]C. Z. Xiao, H. B. Zhuo, Y. Yin, Z. J. Liu, C. Y. Zheng, and X. T. He, "Linear theory of multibeam parametric instabilities in homogeneous plasmas," Phys. Plasmas **26**, 062109 (2019).
[25]Y. Zhao, C. F. Wu, S. M. Weng, Z. M. Sheng, and J. Q. Zhu, "Mitigation of multibeam stimulated Raman scattering with polychromatic light," Plasma Phys. Controlled Fusion **63**, 055006 (2021).
[26]S. J. Yang, H. B. Zhuo, Y. Yin, Z. J. Liu, C. Y. Zheng, X. T. He, and C. Z. Xiao, "Growth and saturation of stimulated Raman scattering in two overlapping laser beams," Phys. Rev. E **102**, 013205 (2020).
[27]D. W. Forslund, J. M. Kindel, and E. L. Lindman, "Theory of stimulated scattering processes in laser-irradiated plasmas," Phys. Fluids **18**, 1002–1016 (1975).
[28]L. Hao, Y. Q. Zhao, D. Yang, Z. J. Liu, X. Y. Hu, C. Y. Zheng, S. Y. Zou, F. Wang, X. S. Peng, Z. C. Li, S. W. Li, T. Xu, and H. Y. Wei, "Analysis of stimulated Raman backscatter and stimulated Brillouin backscatter in experiments performed on SG-III prototype facility with a spectral analysis code," Phys. Plasmas **21**, 072705 (2014).
[29]L. Hao, D. Yang, X. Li, Z. C. Li, Y. Y. Liu, H. B. Cai, Z. J. Liu, P. J. Gu, T. Xu, S. W. Li, B. Li, M. Q. He, S. Z. Wu, Q. Wang, L. H. Cao, C. Y. Zheng, W. Y. Zha, X. S. Peng, Y. G. Liu, Y. L. Li, X. M. Liu, P. Yang, L. Guo, X. H. Jiang, L. F. Hou, B. Deng, P. Wang, S. Y. Liu, J. M. Yang, F. Wang, W. D. Zheng, S. Y. Zou, J. Liu, S. E. Jiang, Y. K. Ding, and S. P. Zhu, "Investigation on laser plasma instability of the outer ring beams on SGIII laser facility," AIP Adv. **9**, 095201 (2019).
[30]J. Qiu, L. Hao, L. H. Cao, and S. Y. Zou, "Collective stimulated Brillouin scattering modes of two crossing laser beams with shared ion acoustic wave," arXiv:2105.12548 (2021).
[31]D. J. Strozzi, E. A. Williams, D. E. Hinkel, D. H. Froula, R. A. London, and D. A. Callahan, "Ray-based calculations of backscatter in laser fusion targets," Phys. Plasmas **15**, 102703 (2008).
[32]R. L. Berger, L. J. Suter, L. Divol, R. A. London, T. Chapman, D. H. Froula, N. B. Meezan, P. Neumayer, and S. H. Glenzer, "Beyond the gain exponent: Effect of damping, scale length, and speckle length on stimulated scatter," Phys. Rev. E **91**, 031103 (2015).
[33]J. F. Drake, P. K. Kaw, Y. C. Lee, G. Schmid, C. S. Liu, and M. N. Rosenbluth, "Parametric instabilities of electromagnetic waves in plasmas," Phys. Fluids **17**, 778–785 (1974).
[34]F. F. Chen, *Introduction to Plasma Physics and Controlled Fusion* (Springer, 1984), Vol. 1.
[35]W. L. Kruer, S. C. Wilks, B. B. Afeyan, and R. K. Kirkwood, "Energy transfer between crossing laser beams," Phys. Plasmas **3**, 382–385 (1996).
[36]P. Michel, W. Rozmus, E. A. Williams, L. Divol, R. L. Berger, R. P. J. Town, S. H. Glenzer, and D. A. Callahan, "Stochastic ion heating from many overlapping laser beams in fusion plasmas," Phys. Rev. Lett. **109**, 195004 (2012).
[37]S. N. Dixit, J. K. Lawson, K. R. Manes, H. T. Powell, and K. A. Nugent, "Kinoform phase plates for focal plane irradiance profile control," Opt. Lett. **19**, 417–419 (1994).
[38]S. H. Glenzer, D. H. Froula, L. Divol, M. Dorr, R. L. Berger, S. Dixit, B. A. Hammel, C. Haynam, J. A. Hittinger, J. P. Holder, O. S. Jones, D. H. Kalantar, O. L. Landen, A. B. Langdon, S. Langer, B. J. MacGowan, A. J. Mackinnon, N. Meezan, E. I. Moses, C. Niemann, C. H. Still, L. J. Suter, R. J. Wallace, E. A. Williams, and B. K. F. Young, "Experiments and multiscale simulations of laser propagation through ignition-scale plasmas," Nat. Phys. **3**, 716–719 (2007).
[39]J. D. Moody, B. J. MacGowan, J. E. Rothenberg, R. L. Berger, L. Divol, S. H. Glenzer, R. K. Kirkwood, E. A. Williams, and P. E. Young, "Backscatter reduction using combined spatial, temporal, and polarization beam smoothing in a long-scale-length laser plasma," Phys. Rev. Lett. **86**, 2810–2813 (2001).
[40]I. Barth and N. J. Fisch, "Reducing parametric backscattering by polarization rotation," Phys. Plasmas **23**, 102106 (2016).
[41]Y. Q. Gao, Y. Cui, L. J. Ji, D. X. Rao, X. H. Zhao, F. J. Li, W. Feng, L. Xia, J. N. Liu, H. T. Shi, P. Y. Du, J. Liu, X. L. Li, T. Wang, T. X. Zhang, C. Shan, Y. L. Hua, W. X. Ma, X. Sun, X. F. Chen, X. G. Huang, J. Zhu, W. B. Pei, Z. Sui, and S. Z. Fu, "Development of low-coherence high-power laser drivers for inertial confinement fusion," Matter Radiat. Extremes **5**, 065201 (2020).
[42]Z. Q. Zhong, B. Li, H. Xiong, J. W. Li, J. Qiu, L. Hao, and B. Zhang, "Effective optical smoothing scheme to suppress laser plasma instabilities by time-dependent polarization rotation via pulse chirping," Opt. Express **29**, 1304–1319 (2021).
[43]P. Michel, L. Divol, E. A. Williams, C. A. Thomas, D. A. Callahan, S. Weber, S. W. Haan, J. D. Salmonson, N. B. Meezan, O. L. Landen, S. Dixit, D. E. Hinkel, M. J. Edwards, B. J. MacGowan, J. D. Lindl, S. H. Glenzer, and L. J. Suter, "Energy transfer between laser beams crossing in ignition hohlraums," Phys. Plasmas **16**, 042702 (2009).
[44]In discussions for zero laser wavelength difference, $90^\circ \geq \varphi_s \geq -90^\circ$ for $\theta_s = 0^\circ$ or $\theta_s = 180^\circ$ is adopted to denote different SL modes. For $\theta_s = 0$, $\alpha_\perp = \arctan(\tan\varphi_s/\sin\theta_h)$, while for $\theta_s = 180^\circ$, $\alpha_\perp = 180 - \arctan(\tan\varphi_s/\sin\theta_h)$. Thus, for $\Delta\lambda_0 = 0$, $\alpha_\perp = 0$ corresponds to "forward" in-plane scattering ($\theta_s = 0$ and $\varphi_s = 0$), $\alpha_\perp = 180^\circ$ corresponds to "backward" in-plane scattering ($\theta_s = 180^\circ$ and $\varphi_s = 0^\circ$), and $\alpha_\perp = 90^\circ$ corresponds to scattering with the largest out-of-plane angle ($\varphi_s = 90^\circ$).